

## Assessment of statistical agreement of three techniques for the study of cut marks: 3D digital microscope, laser scanning confocal microscopy and micro-photogrammetry

MIGUEL ÁNGEL MATÉ-GONZÁLEZ\*, † , JULIA ARAMENDI‡, JOSÉ YRAVEDRA‡, §, RUTH BLASCO||, JORDI ROSELL#, \*\*, DIEGO GONZÁLEZ-AGUILERA\* & MANUEL DOMÍNGUEZ-RODRIGO‡, §

\*Department of Cartography and Terrain Engineering, Polytechnic School of Avila, University of Salamanca, Avila, Spain

†C.A.I. Arqueometry and Archaeological Analysis, Complutense University, Madrid, Spain

‡Department of Prehistory, Complutense University, Madrid, Spain

§IDEA (Institute of Evolution in Africa), Origins Museum, Madrid, Spain

||Centro Nacional de Investigación en Evolución Humana (CENIEH), Burgos, Spain

#Àrea de Prehistòria, Universitat Rovira i Virgili (URV), Tarragona, Spain

\*\*Institut Català de Paleoecologia Humana i Evolució Social (IPHES), Tarragona, Spain

**Key words.** Experimental cut marks, laser scanning confocal microscopy, micro-photogrammetry, statistical agreement, three-dimensional digital microscope.

### Summary

In the last few years, the study of cut marks on bone surfaces has become fundamental for the interpretation of prehistoric butchery practices. Due to the difficulties in the correct identification of cut marks, many criteria for their description and classification have been suggested. Different techniques, such as three-dimensional digital microscope (3D DM), laser scanning confocal microscopy (LSCM) and micro-photogrammetry (M-PG) have been recently applied to the study of cut marks. Although the 3D DM and LSCM microscopic techniques are the most commonly used for the 3D identification of cut marks, M-PG has also proved to be very efficient and a low-cost method. M-PG is a noninvasive technique that allows the study of the cortical surface without any previous preparation of the samples, and that generates high-resolution models. Despite the current application of microscopic and micro-photogrammetric techniques to taphonomy, their reliability has never been tested. In this paper, we compare 3D DM, LSCM and M-PG in order to assess their resolution and results. In this study, we analyse 26 experimental cut marks generated with a metal knife. The quantitative and qualitative information registered is analysed by means of standard multivariate statistics and geometric morphometrics to assess the similarities and differences obtained with the different methodologies.

### Introduction

Taphonomy was first defined as a scientific discipline in the mid-20th century (Efremov, 1940). However, during the 19th century some researchers had already adopted a taphonomic approach. Authors like Knox (1822), Thirria (1833), Tournal (1833), Dawkins & Boyd (1874) or Harlé (1892) observed and analysed bone surface modifications that appeared in Paleolithic deposits. For instance, early examinations of modern captive carnivores led to the conclusion that some old bone accumulations could be the result of the action of carnivores (Thirria, 1833; Tournal, 1833; Dawkins & Boyd, 1874). Cut marks were also investigated as possible evidence of human modification of animal carcasses (Lartet, 1860). In later studies, Lartet & Christy (1875) and Martin (1906, 1907–1910, 1909) investigated the relationship between butchery patterns and cut marks.

Subsequently, during the second half of the 20th century, taphonomy developed integrating a variety of highly specialised methods. One of these methods is based on the study of cut marks. The initial works of Binford (1981), Bunn (1981) and Shipman (1981) laid the foundation of the investigation and current debate on cut marks. Since Martin's (1906, 1907–1910) early studies and during the whole 20th century (White, 1952, 1953, 1954, 1955; Binford, 1981; Bunn, 1981; Shipman, 1981), three independent research lines have been defined for the study of cut marks. The first line of research focuses on the behavioural functionality of the marks according to their location. The activities that led to the creation of the cut marks can be determined based on their anatomical

Correspondence to: Miguel Angel Maté-González, Department of Cartography and Terrain Engineering, Polytechnic School of Avila, University of Salamanca, Hornos Caleros 50, 05003 Avila, Spain. Tel: 920 35 35 00; e-mail: mategonzalez@usal.es

distribution. A specific location of marks corresponds to different activities, such as filleting, disarticulation, evisceration or skinning (see Binford, 1981; Lyman, 1987; Nilsen, 2001; Galán & Domínguez-Rodrigo, 2013; Bello *et al.*, 2016). The second research line focuses on the behavioural meaning of the frequency of marks. The amount of cut marks on any given assemblage varies according to different circumstances (e.g., Domínguez-Rodrigo & Yravedra, 2009). Nevertheless, the combination of frequencies along with the anatomical distribution of marks has been key to discern early access to carcasses by hominins (Domínguez-Rodrigo *et al.*, 2007). Experimental works in this line (Domínguez-Rodrigo, 1997a,b,c; Lupo & O'Connell, 2002) have been useful as reference to differentiate ancient anthropogenic carcass exploitation strategies. The third line of research of cut marks is based on their identification and characterisation. From the 1980s, several experimental studies have attempted to define the characteristics of cut marks and to differentiate them from other types of alterations such as tooth scores or trampling (Martin, 1907–1910; Walker & Long, 1977; Binford, 1981; Shipman, 1981, 1988; Shipman & Rose, 1983; Andrews & Cook, 1985; Behrensmeier *et al.*, 1986; Olsen & Shipman, 1988; Fiorillo, 1989; Cruz Uribe & Klein 1994; Fisher, 1995; Blasco *et al.*, 2008; Domínguez-Rodrigo *et al.*, 2009, 2010).

Studies focused on the determination of the type of tools or raw materials used to generate cut marks have also become relevant. Notable among these works are those that seek to differentiate cut marks produced with metal knives from those generated by stone tools (Olsen, 1988; Greenfield, 1999, 2004, 2006a,b; Bello & Soligo, 2008; Yravedra *et al.*, 2009), shell (Choi & Driwantoro, 2007), or bamboo (Spennerman, 1990; West & Louys, 2007; Bonney, 2014), or the studies that try to distinguish between lithic tool types including simple or retouched flakes and hand-axes (Walker, 1978; Shipman & Rose, 1983; Bello *et al.*, 2009; Domínguez-Rodrigo *et al.*, 2009; De Juana *et al.*, 2010; Galán & Domínguez-Rodrigo, 2013).

Techniques based on microimages are essential in order to get high-resolution data that allow the identification of the type of tool or raw material used. In these studies, cut mark morphology analyses have been studied using different techniques, such as optic microscopy, hand lenses and scanning electron microscope (SEM) and environmental scanning electron microscope (ESEM) (Shipman, 1981; Olsen, 1988; Greenfield, 1999, 2004, 2006a,b; Smith & Brickley, 2004; Lewis, 2008; Blasco *et al.*, 2016), binocular microscope for high-resolution pictures (Domínguez-Rodrigo *et al.*, 2009; De Juana *et al.*, 2010; Marín-Monfort *et al.*, 2014), digital imaging techniques (Gilbert & Richards, 2000), three-dimensional (3D) reconstruction (During & Nilsson, 1991; Bartelink *et al.*, 2001; Kaiser and Katterwe, 2001), 3D digital microscope (Boschin & Crezzini, 2012; Crezzini *et al.*, 2014), Alicona 3D Infinite Focus Imaging microscope (Bello & Soligo, 2008; Bello *et al.*, 2009; Bello, 2011; Bonney, 2014), laser scanning confocal microscopy (LSCM) (Archer & Braun, 2013) or

micro-photogrammetric techniques (M-PG) (Maté-González *et al.*, 2015, 2016).

All of these techniques have been applied to the analysis of cut marks, but no comparative studies have been conducted to date to test their comparative reliability in the reconstruction of mark section morphology and dimensions. In the present study, we selected a sample of cut marks on different bones and analysed them using 3D DM, LSCM and M-PG in order to assess the resolution of each technique and see if their results are consistent. This has major repercussions for the correct adscription of mark types to agencies and also for the accuracy in identifying cut marks from other types of bone surface modifications.

### Method and sample

The sample consists of 26 cut marks, which have been documented using three different techniques: 3D DM, LSCM and M-PG. A total of 78 profiles (three homologous profiles for each cut mark) have been generated in order to create a comparable sample (see below). In all cases, cut marks were measured at mid-length (about 50% of the mark length) as suggested in Maté-González *et al.* (2015). According to this work, for a confident comparison of cut marks, the values for the sections between 30% and 70% of the mark length would be the most representative ones. The marks were located on three diaphyses of long bones from a young *Ovis aries* individual (Fig. 1) The age of the individual might be a modifying variable in some cases, but taking into account that the sample used in this study is homogeneous, the age of the prey does not alter the final result.

Cut marks were made with a stainless steel knife model Molybdenum Vanadio C 0.5 CR 14 MO 0.5 VA 0.25 (Fig. 1). The use of a stainless steel knife allows the control of certain variables, because the tool edge characteristics always stay



Fig. 1. Stainless steel knife used in the study to create the cut marks on several bones.

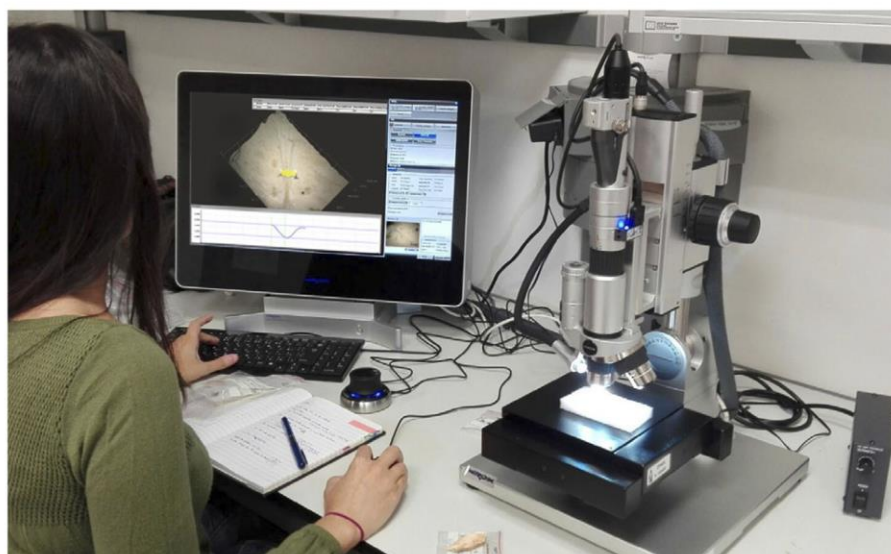


Fig. 2. KH-8700 3D digital microscope in the IPHES, Institut català de Paleoeologia Humana i Evolució Social, Tarragona, Spain.

stable, contrary to other materials such as flint, quartzite or basalt.

All experiments cut marks were made by the same person and the measurements of cut marks of the bones, were made in the same point of cut marks, all techniques analysed the same part of cut mark.

#### *Three-dimensional digital microscope*

Cut marks were observed using the KH-8700 3D digital microscope (3D DM) located at IPHES – Catalan Institute of Human Paleoeology and Social Evolution, Tarragona, Spain (Figs. 2 and 3). This microscope uses high-intensity LED optics with a full HD monitor to reconstruct 3D surfaces (Table 1). Its integrated stepping motor allows for an accurate scanning with  $0.05 \text{ } \mu\text{m pulse}^{-1}$  precision and 30 mm of automated travel distance. 3D profiles were generated using a direct overhead light source (LED lamp) and taking a sequence of frames at a specified interval to record changes over the set duration. In our case a total of 25–30 photos were taken for each cut mark. The number of photos was manually determined according to the bone morphology and incision characteristics, such as shape, angle and/or depth. The KH-8700 software allowed us to take images at different elevations and complete the 3D profiles within a temporal range of approximately 20–30 s. The time spent varied according to the number of photos acquired in each case. It is important to note that data collection for cross-sectional profiles depends largely on the intensity and incidence of light. For this reason, it is necessary that the light distribution is uniform on all the area to be scanned. This is sometimes complicated because the depth of some cut marks prevents the light from reaching all points in the same way.

The resulting 3D images show a high optical resolution and a wide field of view simultaneously.

#### *Laser scanning confocal microscopy*

Cut marks were also recorded using an Olympus LEXT OLS3000 Confocal Laser Microscope (Figs. 4 and 5) at CENIEH – National Research Centre of Human Evolution, Burgos, Spain (Table 2). This microscope is equipped with a 408 nm laser, providing high-resolution images of specific cut mark sections. The motorised stage also provides information from several parameters such as roughness, size and/or shape that is used to generate the 3D reconstructions of transversal sections. The use of the laser allows a real reading of the bone topography, including cut mark transversal morphology, and avoids problems of data collecting derived from the intensity and/or incidence of direct light, such as brightness or shadows. However, the resulting 3D image resolution and quality is not as accurate (including the colour and texture changes) as the one generated by KH-8700 3D Digital Microscope. For data collection, the number of photos was set by default, not exceeding in any case 87 automated steps. Each 3D model and cross-sectional profile for specific points of the cut mark took approximately 40–60 s.

#### *Micro-photogrammetry*

Finally, micro-photogrammetry (M-PG) and computer visualisation techniques were used to create high-resolution 3D models of cut mark sections. Precise metrical models were generated using images taken with oblique photography using a CANON EOS 700D (Fig. 6) with a 60 mm macrolens

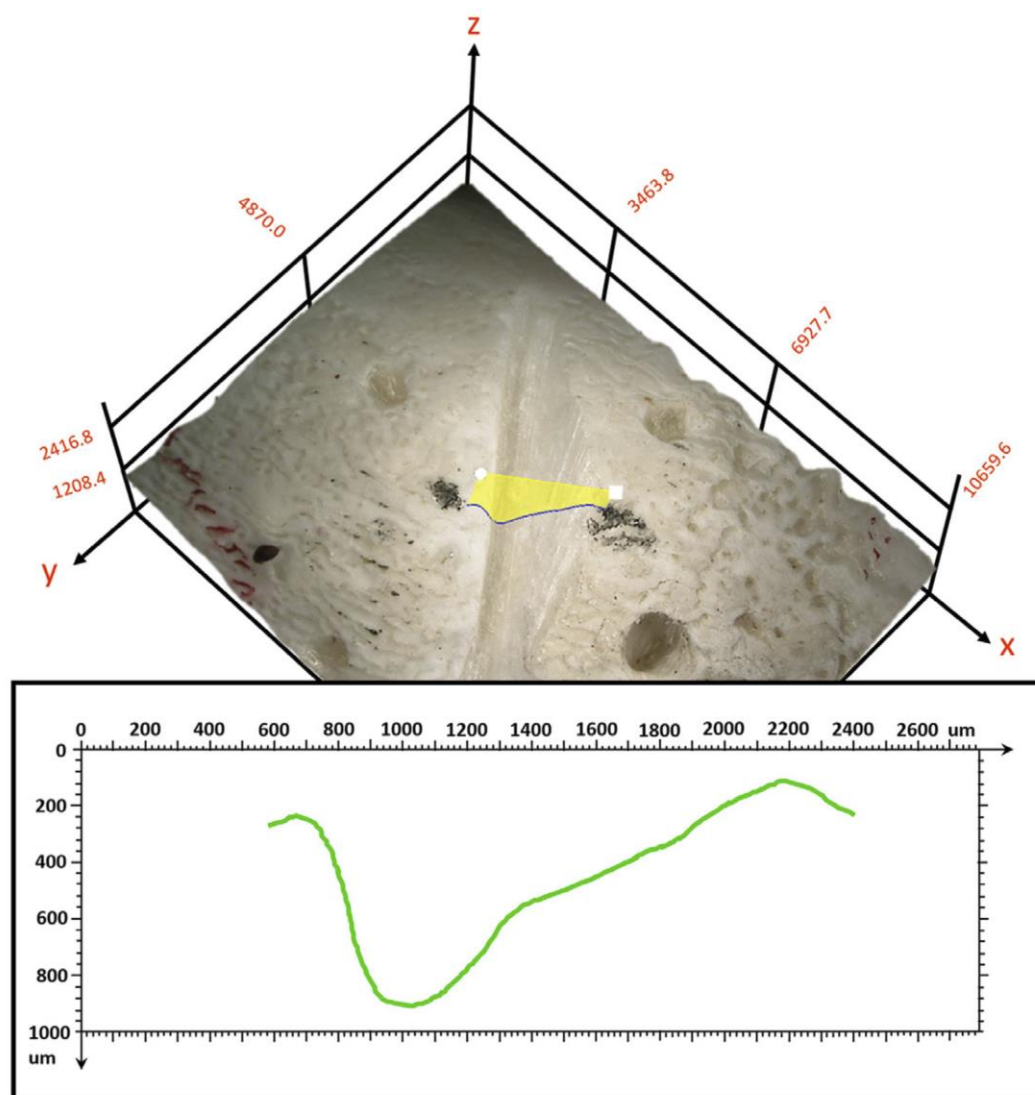


Fig. 3. Data collection and profile generation using the KH-8700 3D digital microscope.

Table 1. Technical specifications of the KH-8700 3D digital microscope.

KH-8700 3D digital microscope	
Type	KH-8700
Sensor size	7.18 × 5.32 mm, 2.11 MP CCD sensor
Pixel size	0.248 (H) × 0.248 (V) mm
Image size	225 MP – 15 000 pixels (H) × 15 000 pixels (V) (tiling image)
Total pixels	2.11 MP 1688 (H) × 1248 (V)
Focal length	10 mm
Focused distance to object	8.71–1.22 mm

(Table 3) and following the specified protocol explained in Maté-González *et al.* (2015). The camera was self-calibrated to simultaneously compute the interior and exterior camera parameters (Fraser, 1980). For data collection, a total of 9–13 photos were taken for each mark. The number of photos varied depending on the geometry of the bone and the shape of the mark. The 3D reconstruction of each mark took 30–40 min depending on the final number of photos acquired. Photographs were processed with an open-source photogrammetric reconstruction software GRAPHOS (inteGRated PHotogrammetric Suite) (González-Aguilera *et al.*, 2016a,b) to generate a 3D model for each mark. After producing scaled 3D models, Global Mapper software was used to define and measure mark profiles.

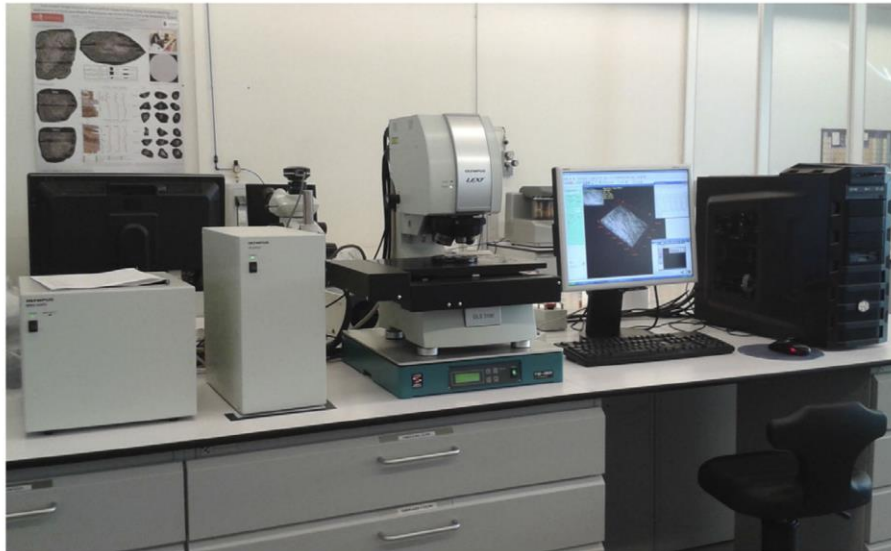


Fig. 4. Olympus LEXT OLS3000 confocal laser microscope in the Microscopy Laboratory of the CENIEH, Centro Nacional de Investigación sobre la Evolución Humana, Burgos, Spain.

#### Multivariate statistical analysis

A series of measurements (Fig. 7) were taken on each digital model of the mark sections (see Fig. S1). The free software tpsDig2 (v. 2.1.7) was used to measure the width of the incision at the surface (WIS), the width of the incision at the mean (WIM), the width of the incision at its bottom (WIB), the opening angle of the incision (OA), the depth of the incision (DB), the left depth of the incision convergent (LDC) and the right depth of the incision convergent (RDC) (*sensu Bello et al.*, 2013).

Measurements were imported into the free software R ([www.rproject.org](http://www.rproject.org), Core-Team, 2015). In order to test if there was any difference in the measurements obtained with each methodology, several statistical tests were performed. First, variance analyses (ANOVA and MANOVA) were applied to statistically assess the presence of separate groups by comparing their means. The Levene's test for homogeneity of variance was included. This test is used to assess equality among two or more sample variances and the feasibility of variance analyses. Second, a multivariate principal components analysis (PCA) of the biometric data was performed. The PCA is a commonly used method for simplification of a large set of variables to few dimensions, and assess patterns of variation among the data. The PCA estimates similarities and differences of marks on a bidimensional Euclidean space and in the present study we used the mark measurements transformed through scaling.

#### Geometric morphometric analysis

A geometric morphometric analysis was performed as a supplementary alternative to the multivariate metric analysis.

In this case, seven homologous points (landmarks) per section – as shown in Figure 7 (LM 1–7) – were considered from each mark. Landmarks were digitalised using tpsUtil (v. 1.60.) and tpsDig2 (v. 2.1.7), as explained in Maté-González *et al.* (2015). The location of the landmarks responded to the measures considered for the statistical analysis. LandMark 1 (LM) was found at the beginning of the left line in the mark section; LM2 appeared in the middle of this line; LM3 was placed approximately at 10% of the right end of the mark; LM4 was at the very end; LM5, LM6 and LM7, in an opposed position to LM3, LM2 and LM1, respectively (Fig. 7). The resulting tps files were edited and imported into MorphoJ (Klingenberg, 2011) to perform the geometric morphometric analysis. MorphoJ is an integrated free software for geometric morphometrics that supports 2D and 3D data. The program was designed for the analysis of biological data, thus it performs better with samples that do vary extremely, as it is the case in this study. MorphoJ geometric morphometric analysis is based on a full Procrustes fit and an orthogonal tangent projection (Dryden & Mardia, 1998) that prepares the sample for usual multivariate statistical analyses.

The seven landmarks digitalised for the whole sample and the three methodologies were first subjected to a general procrustes analysis (GPA). This technique normalises the form information by the application of superimposition procedures. This involves the translation, rotation, and scaling of shapes defined by landmark configurations. After the standardisation of the data, there are always some remaining differences that expose patterns of variation and covariation between structures that after being projected into a flat Euclidean space

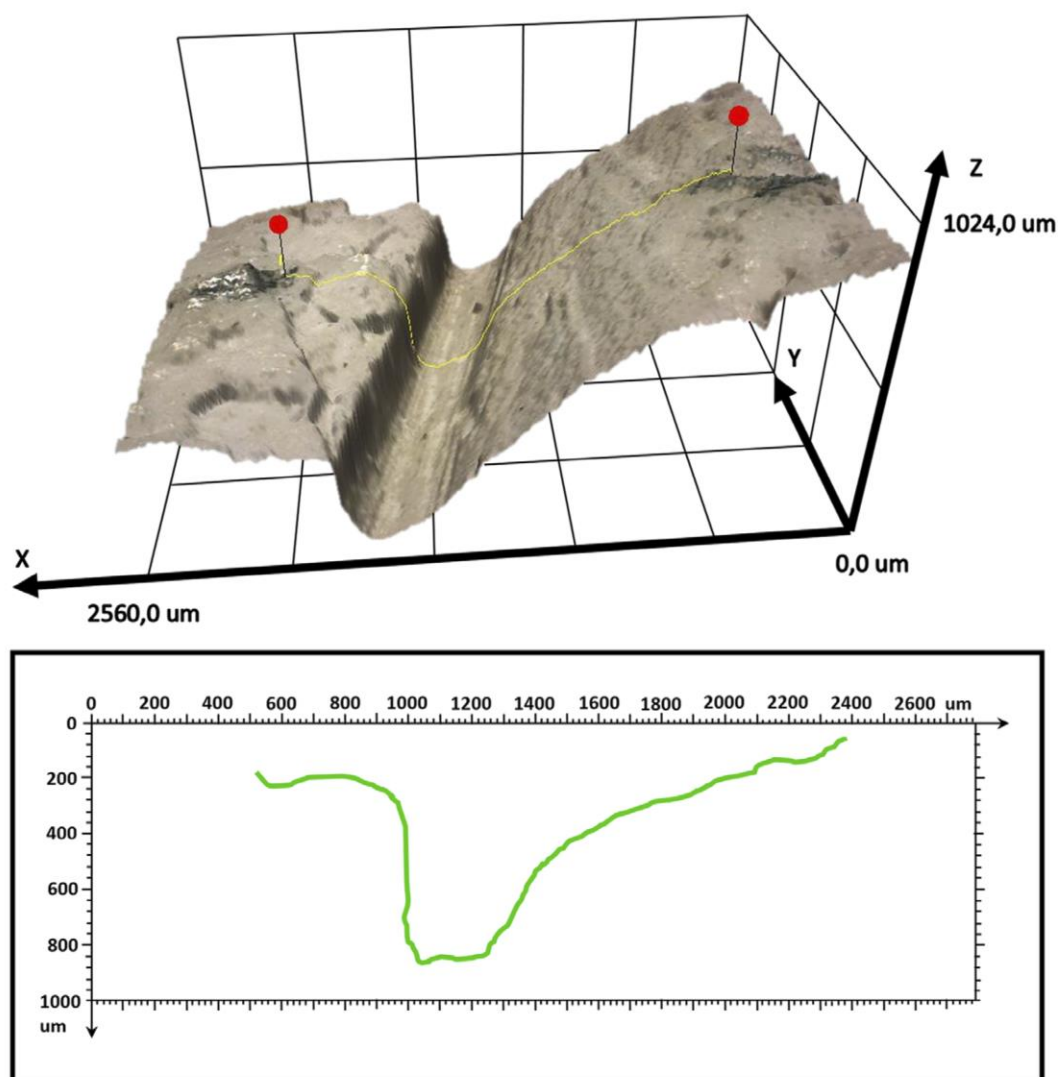


Fig. 5. Data collection and profile generation using the Olympus LEXT OLS3000 confocal laser microscope.

**Table 2.** Technical specifications of the Olympus LEXT OLS3000 confocal laser microscope.

Olympus LEXT OLS3000 confocal laser microscope	
Type	LEXT OLS3000 Circle pinhole + photomultiplier
Sensor size	0.12 $\mu\text{m}$ and 0.01 $\mu\text{m}$ Z resolution
Pixel size	12 $\mu\text{m}$
Image size	1024 $\times$ 1024 pixels (for confocal image) 1024 $\times$ 768 pixels (for confocal + colour image)
Total pixels	1 MP (for confocal image) 0.7 MP (for confocal + colour image)
Focal length	10–45 mm
Focused distance to object	5–20 mm

can be analysed by means of common multivariate statistics (Slice, 2001; Rohlf, 1999). A PCA in shape space, where only differences in shape excluding size variables are taken into account, was performed for the three samples. PCA scores were later exported and examined for variance: a MANOVA and an ANOVA tests using the Levene's test for equality of variances was performed in R.

### Experimental results

The statistical tests applied on all these models show different results, even if the measurements used were always the same (Fig. 7).

The results obtained with MANOVA (Table 4) highlight a significant difference ( $p < 0.05$ ) between the biometric

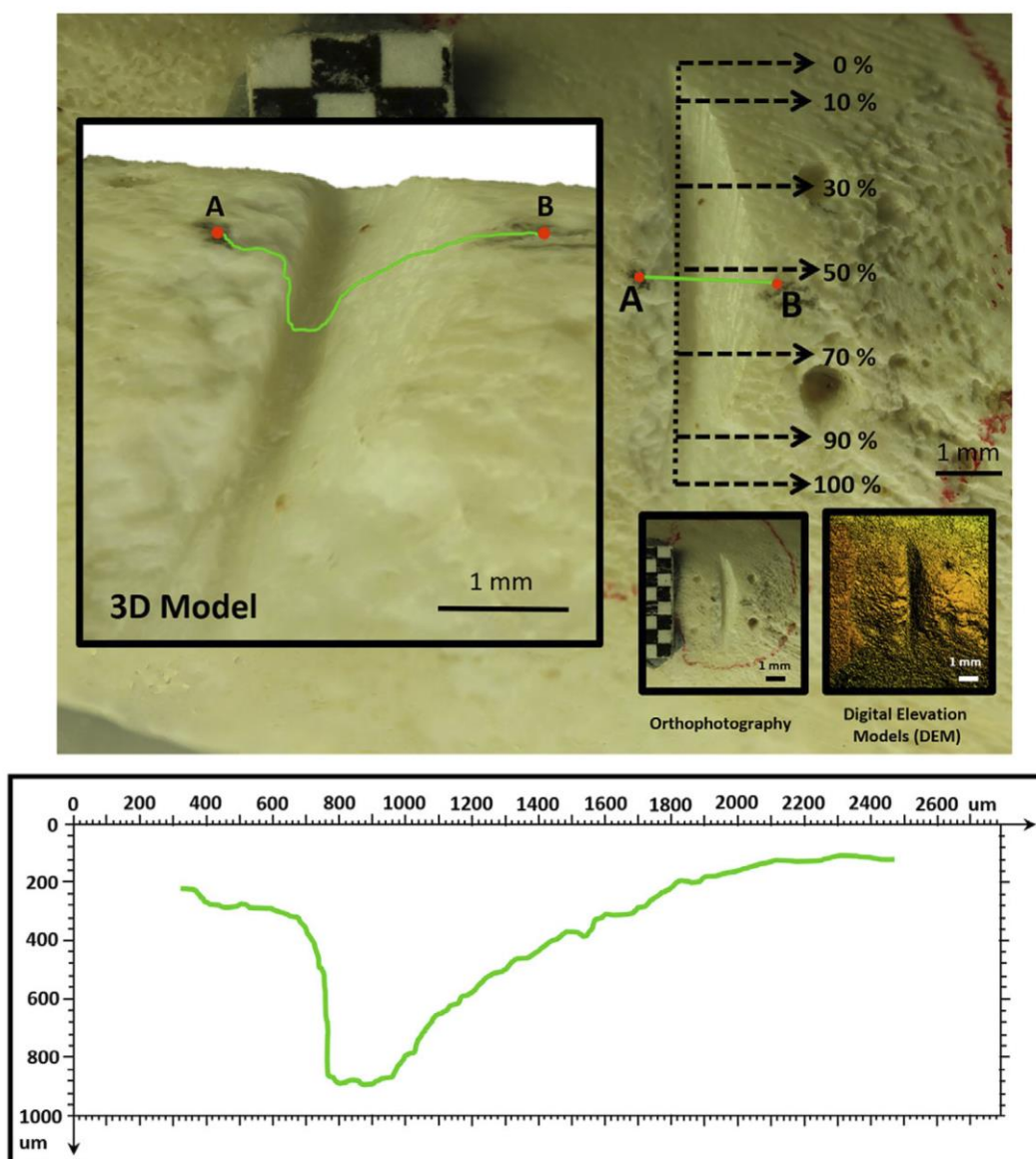


Fig. 6. Data collection and profile generation using micro-photogrammetry.

Table 3. Technical specifications of the photographic sensor with macrolens (Canon EOS 700D).

Canon EOS 700D	
Type	CMOS
Sensor size	22.3 × 14.9 mm
Pixel size	4.3 μm
Image size	5184 × 3456 pixels
Total pixels	18.0 MP
Focal length	60 mm
Focused distance to object	100–120 mm

measurements obtained with 3D DM and the measurements taken on the models generated by means of M-PG and LSCM, whereas the latter pairwise comparison is similar.

More specifically, when comparing results using single variables at a time the ANOVA (Table 5) and Levene's tests (Table 6) suggest that such differences are not that important. Indeed, the main differences between microscope pairs seem to be focused on the opening angle of the incision (OA) (Tables 5 and 6). The rest of the measurements on the other variables do not allow the distinction between techniques.

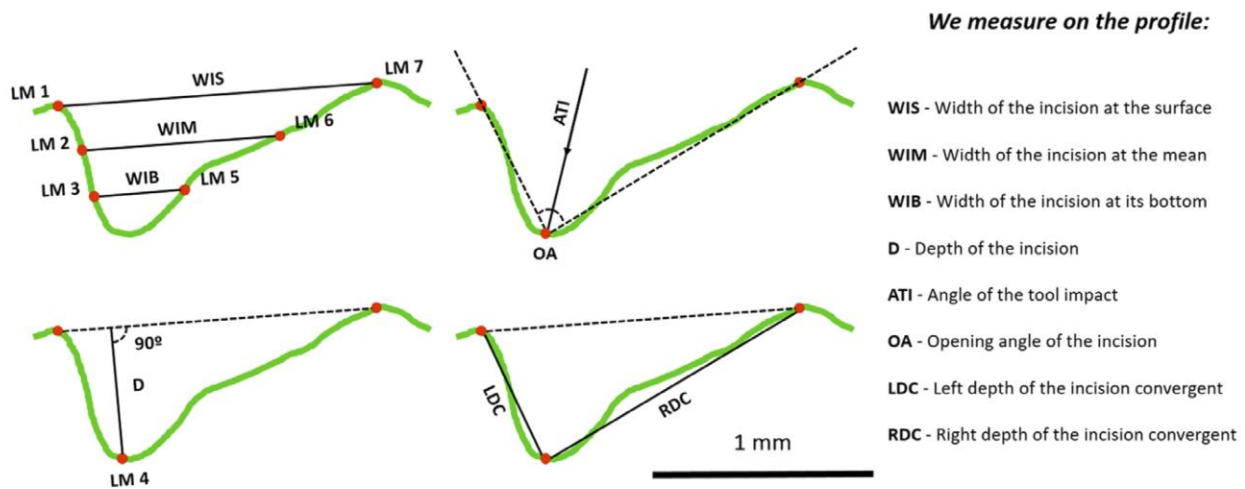


Fig. 7. Location of measurements sensu Bello *et al.* (2013). Landmarks (LM1–7) used for the morphometric model are also represented.

Table 4. Pairwise MANOVA results of the raw metric data.

M-PG – LSCM	0.53008
LSCM – 3D DM	0.030327
3D DM – M-PG	0.0049477

A principal component analysis (PCA) using raw metrics was also performed to compare the cut mark models generated with each technique (Fig. 8). The 95% confidence

ellipses of each microscope type overlap with one other, especially those corresponding to the cut marks registered with micro-photogrammetry (Fig. 8, in red) and LSCM (Fig. 8, in green). The cut marks documented with 3D DM (Fig. 8, in black) mostly fall within the space described by the other two methods, but are located in the upper part of the second component. The cut marks are mostly explained by the first two Principal Components (PCs – 85.8% of the total variance). Although PC1 (63.9%) seems to be determined by

Table 5. ANOVA results using single variables of the raw metric data.

	3D DM vs. M-PG vs. LSCM		3D DM vs. LSCM		3D DM vs. M-PG		M-PG vs. LSCM	
	F	p Value	F	p Value	F	p Value	F	p Value
WIS	1.882	0.159	2.912	0.094	2.749	0.104	0.008	0.929
WIM	1.436	0.244	1.879	0.177	2.345	0.132	0.021	0.886
WIB	1.794	0.173	0.489	0.488	3.611	0.063	1.450	0.234
D	0.840	0.436	1.263	0.266	1.228	0.273	0.004	0.949
LDC	0.044	0.957	0.035	0.853	0.011	0.915	0.078	0.781
RDC	0.080	0.924	0.151	0.699	0.052	0.820	0.030	0.864
OA	7.457	0.001	11.520	0.001	7.952	0.007	0.244	0.624

Table 6. Results of Levene's test for equality of variance using single variables of the raw metric data.

	3D DM vs. M-PG vs. LSCM		3D DM vs. LSCM		3D DM vs. M-PG		M-PG vs. LSCM	
	Levene's test	p Value	Levene's test	p Value	Levene's test	p Value	Levene's test	p Value
WIS	0.110	0.896	0.211	0.648	0.051	0.822	0.062	0.805
WIM	0.065	0.938	0.121	0.730	0.025	0.875	0.044	0.835
WIB	0.267	0.767	0.079	0.779	0.162	0.689	0.739	0.394
D	0.139	0.870	0.001	0.979	0.230	0.634	0.194	0.661
LDC	0.445	0.643	0.478	0.493	0.054	0.818	0.700	0.407
RDC	0.043	0.958	0.004	0.950	0.043	0.836	0.089	0.767
OA	2.941	0.059	5.193	0.027	2.228	0.142	0.707	0.405



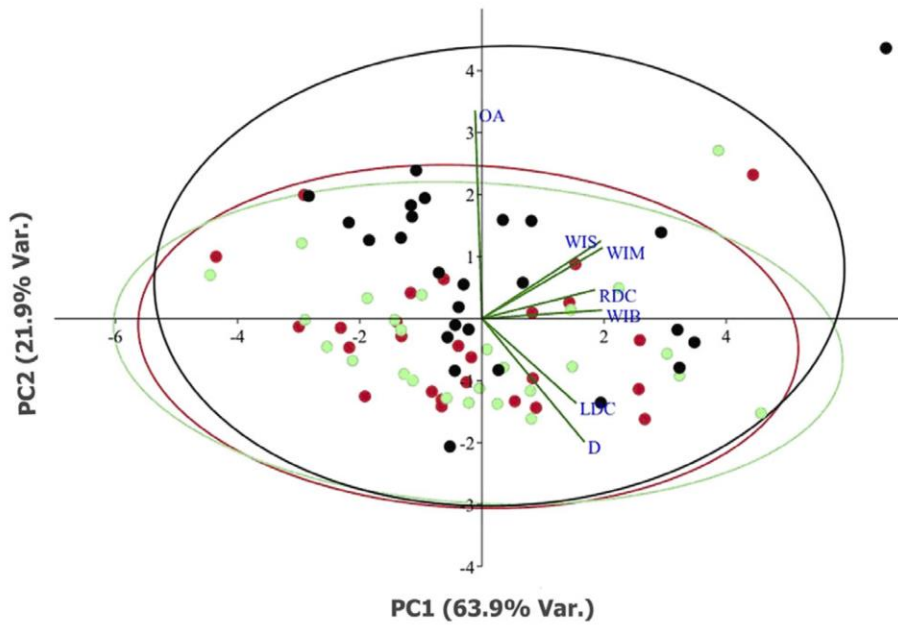


Fig. 8. Principal components analysis (PCA) of the biometric measurements taken on the cut marks models generated using micro-photogrammetric methods (red), LSCM (green) and 3D DM (black).

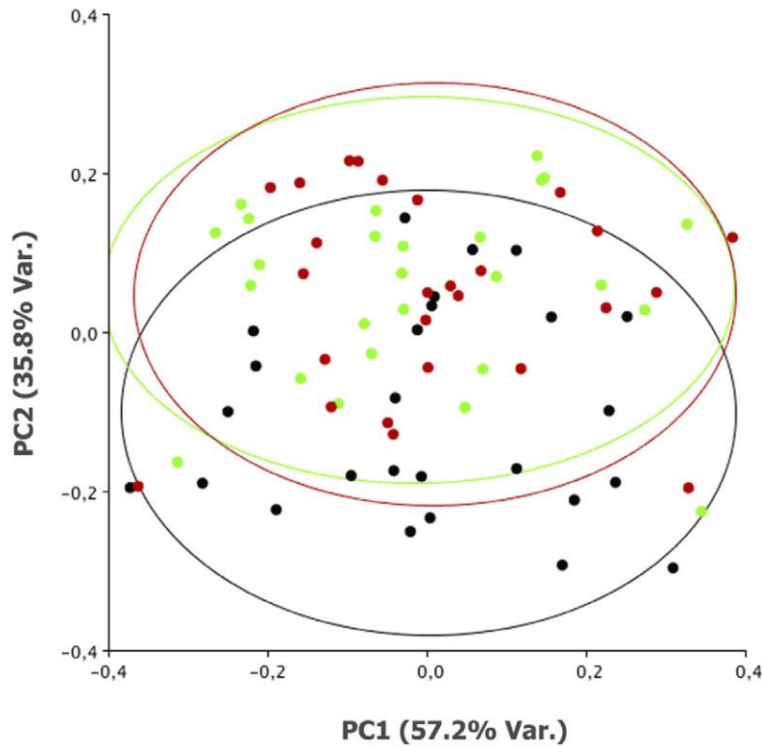


Fig. 9. Morphometric principal components analysis (PCA) after standardisation by means of GPA. Groups corresponding to the different techniques are highlighted in colours: M-PG (red), LSCM (green) and 3D DM (black).

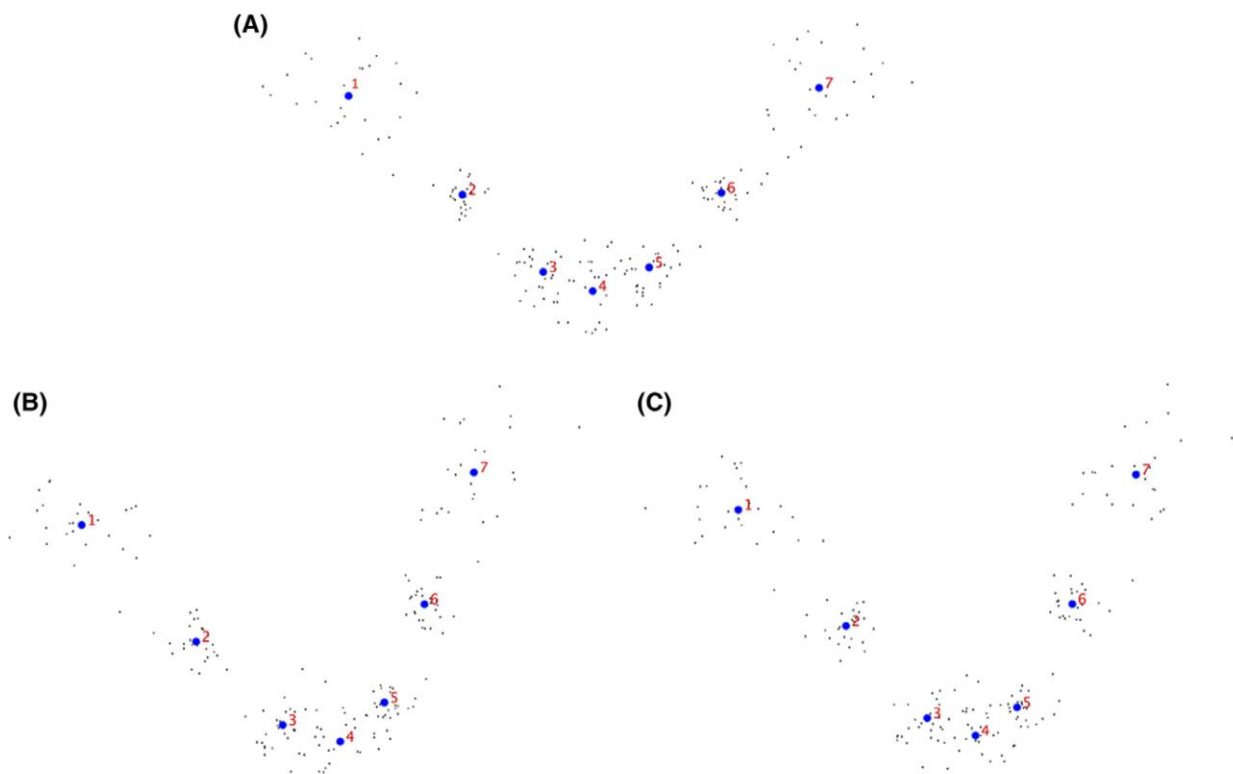


Fig. 10. Silhouettes of cut marks using (A) 3D DM, (B) LSCM and (C) M-PG. The blue points are the centroids associated to each landmark

Table 7. Pairwise MANOVA results of the morphometric data.

M-PG – LSCM	0.72165
LSCM – 3D DM	0.00059659
3D DM – M-PG	0.0030465

the action of most measurements (especially by the width of the incision at its bottom – WIB), PC2 (21.9%) is mostly explained by the opening angle of the incision (OA). Despite the similarities, it is possible to observe a trend towards larger measurements in the cut marks registered with 3D DM.

The geometric morphometric bidimensional analysis of the seven landmarks supports the biometric results. After the GPA, a PCA was conducted (Fig. 9). The three groups of cut marks overlap considerably in the PCA plot where 92.98% of the total variance is explained. However, a slight difference can be noticed, as cut mark models generated using 3D DM show larger values than the other two groups. Marks generated with the electronic microscope are wider and shallower than those generated using the LSCM and M-PG techniques (Fig. 10).

Variance analyses (MANOVA, ANOVA and Levene's test) conducted on the PC scores, support the results obtained with the raw metric data. Although the MANOVA (Table 7) shows

a significant difference between 3D DM and the other two techniques, the ANOVA ( $F = 0.8782$ ,  $p = 0.453$ ) and the Levene's test for homogeneity of variance ( $p = 0.08126$ ) do not allow the rejection of the null hypothesis for equal means. However, the Levene's test is closer to the 5% significance level.

## Discussion

The present analysis compares three different techniques recently used for the study of taphonomic marks (namely, cut marks) on cortical surfaces. We have observed that the three methods present similar results and are, thus, equally valid for taphonomic metric and morphometric analyses. Although Pante *et al.* (2017) qualified the M-PG method as more inaccurate and prone to error, this prejudiced statement was not supported by any data. Here we show that M-PG meets the standards of more costly and technologically more sophisticated techniques, such as the use of LSCM, and M-PG may even exceed the quality of the results obtained via 3D DM.

The results obtained using the KH-8700 3D Digital Microscope differ slightly (especially in some measurements) from those using the Olympus LEXT OLS3000 Confocal Laser Microscope and the CANON EOS 700D-based M-PG techniques. Differences could be due to the different level of detail

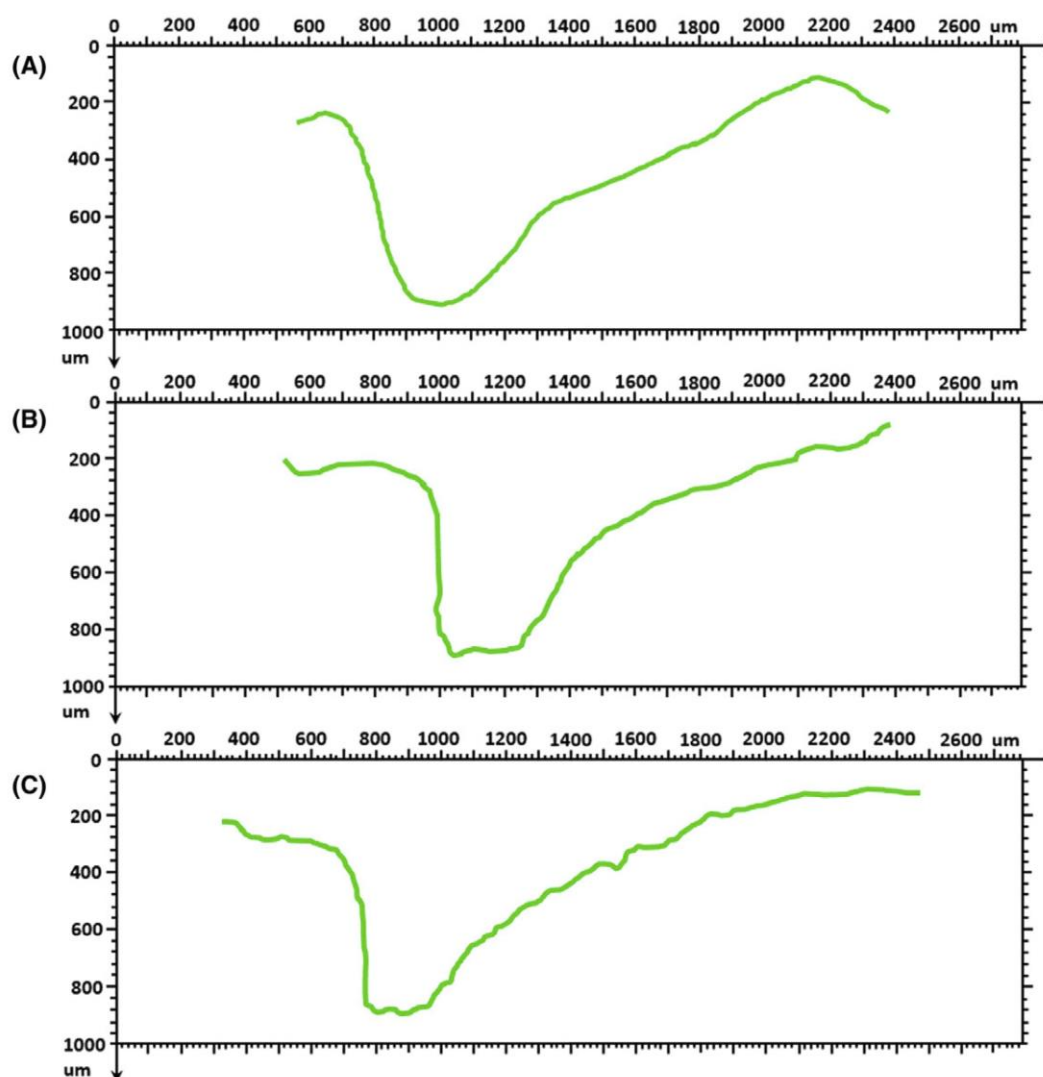


Fig. 11. Homologous profiles of the same cut mark generated with (A) 3D DM, (B) LSCM and (C) M-PG, where the different level of detail generated by each method can be appreciated.

generated by each method. Although M-PG and LSCM produce high-resolution and very detailed profiles, 3D DM provides less detail. In fact, the ground sample distance (GSD) computed for each technique confirms this aspect: 3D DM- $30\ \mu\text{m}$ , LSCM- $6\ \mu\text{m}$  and M-PG- $7\ \mu\text{m}$ . A less detailed reproduction of the mark profile may vary the location of the landmarks according to their definition (e.g. the end point of the cut mark) as the observer is not able to fully notice the features of the walls that define the limit of the mark (Fig. 11). The lack of details or the major differences in some of the profiles extracted using 3D DM could be due to the data collection process using this kind of microscopes (see differences in the mean profile in Fig. 10). The profile images are created taking a sequence of frames depending largely on the intensity and incidence of

light. That means that depending on the lighting the image might vary, so it depends on the observer.

Surprisingly, the low-cost M-PG method, based on the use of a digital camera equipped with 60 mm macrolenses and an open-source photogrammetric software, provides a very good resolution (GSD -  $7\ \mu\text{m}$ ) and the best level of detail among the three techniques (see the profile in Fig. 11). Although the results obtained in this study are very satisfactory and prove the validity of this low-cost method for the study of conspicuous and well defined marks (e.g. cut marks, scores, pits) as demonstrated by Arriaza *et al.* (2017), Maté-González *et al.* (2016) and Yravedra *et al.* (2017), M-PG might not be valid for the study of inconspicuous and vaguely defined marks (e.g. trampling) where the camera may lack

enough resolution to capture the subtleties of fine microscopic details.

The time required for the reconstruction of the marks is short with the three methods analysed in this study. However, M-PG takes more time (around 25 min) than the other two techniques (few seconds). Time differences do not seem to be of such importance to prioritise the expensive methods. In any case, researchers should bear this aspect in mind before choosing the technique for the virtual reconstruction of marks.

In essence, M-PG is a very useful low-cost method which overcomes the limitations implied in the use of microscopes – that is restricted access due to high costs – by reducing analytical costs and, consequently, enlarging the sample to be tested.

Recent research has shown the advantages of obtaining 3D images for the study of taphonomic marks (Bello, 2011, 2013; Boschini & Crezzini, 2012), Paleolithic engravings (Güth, 2012) or Roman pottery graffiti (Montani *et al.*, 2012). Some authors especially highlight the potential of high-resolution 3D studies for the identification of different taphonomic processes (Pante *et al.*, 2017). Using a confocal profilometry, Pante *et al.* (2017) have distinguished between tooth and cut marks. However, this study, although well-intentioned, presents some problems. First, there is no actual need to use 3D analyses to differentiate cut marks from tooth marks, because these marks are easily distinguishable using 10× magnification lenses (Blumenschine *et al.*, 1996). The study would have been more interesting if this technology would have been applied to differentiate agents using a specific type of mark – for example tooth marks produced by different classes of carnivores – or to determine the raw materials used in the exploitation of carcasses on the basis of cut marks or even more relevant, if cut marks were efficiently differentiated from trampling marks and other marks resulting from sedimentary abrasion. Recent micro-photogrammetric and morphometric analyses have approached agency in the determination of carnivore bone modifications, on the basis of tooth scores on bones (Arriaza *et al.*, 2017; Yravedra *et al.*, 2017), as well as the raw materials used in the processing of carcasses through the morphometric analysis of cut marks (Maté-González *et al.*, 2016; Yravedra *et al.*, 2017).

Recently, Pante *et al.* (2017) argued that the new wave of taphonomic studies based on the 3D reproduction of marks should be based on easily available (e.g. low cost) and replicable methods. Here, we have presented a method that clearly meets both needs. The results presented here prove that 3D DM, LSCM and M-PG are more or less equally effective and therefore comparable. Therefore, it would be possible to conduct integrated taphonomic projects to assess mark variability based on different variables such as animal size (Bello *et al.*, 2013), raw material (Maté-González *et al.*, 2016; Yravedra *et al.*, 2017), or tool type (Galán & Dominguez-Rodrigo, 2013; Yravedra *et al.*, 2017) regardless of the technique. Some studies along this research line are already published (Bello &

Soligo, 2008; Bello, 2011; Bello *et al.*, 2013, 2015), and they could establish the foundations of future analyses integrating different works using diverse techniques; for example Alicone 3D (Bello & Soligo, 2008; Bello, 2011; Bello *et al.*, 2013), ESEM (Bello *et al.*, 2015; Blasco *et al.*, 2016) M-PG (Maté-González *et al.*, 2016; Yravedra *et al.*, 2017) and LSCM (Archer & Braun, 2013). Future analyses should also include the 3D morphometric and biometric study of the marks. This tool would be especially useful in the case of tooth pits where the extraction of a bidimensional profile might be ignoring important information.

## Conclusions

This study has demonstrated that three of the modern analytical techniques recently used for the study of cut marks produced overall statistically similar results and are equally valid for the study of bone surface modifications. Although some small differences have been observed between 3D DM, LSCM and M-PG, they are not important. Particularly surprising is the high degree of similarity between LSCM and M-PG, showing that both completely unrelated techniques can produce statistically indistinguishable results.

The similarity between these techniques allows the comparison of studies using different approaches or techniques. The different methodologies for the 3D modelling of marks can also benefit from the interaction of these techniques. For example, M-PG is a very fast, cheap and useful technique for the study of conspicuous cut or tooth marks in large samples, but it does not have sufficient resolution to analyse trampling marks. On the contrary, LSCM and 3D DM are not as easy available methods because they are expensive, but allow the study of inconspicuous marks thanks to its higher magnification and resolution level. Certain 3D modelling software types, like Alicona, have also shown their high performance, whereas the application of the Confocal Profilometry is still rather anecdotal and its reliability has not been proved yet by testing similar marks (e.g. cut marks made with different tools or raw materials or trampling marks compared to cut marks). For its part, GRAPHOS is distributed through an open source platform (<https://github.com/itos3d/GRAPHOS/releases>) for research and educational needs. It should be remarked that, up to date, there is not any open source photogrammetric GUI for the scientific community which encloses the modern pipeline of close-range photogrammetry and computer vision.

The compatibility of the three methods used in this study and the possibility of producing comparable high-resolution 3D models using any of them facilitates the future study of taphonomic bone modifications.

## Acknowledgements

We would like to thank the TIDOP Group from the Department of Cartographic and Land Engineering of the High

Polytechnics School of Avila, University of Salamanca, for the use of tools and facilities. We want to recognise the technical support provided by C.A.I. Arqueometry and Archaeological Analysis from Complutense University, which has been very useful to carry out the present work. J. Rosell and R. Blasco develop their work within the Spanish MINECO/FEDER projects CGL2015-65387-C3-1-P (J. Rosell) and CGL2015-68604-P (R. Blasco), the Generalitat de Catalunya-AGAUR projects 2014 SGR 900 and 2014/100573, and the SENECA Foundation project 19434/PI/14.

## References

- Andrews, P. & Cook, J. (1985) Natural modifications to bones in a temperate setting. *Man* **20**, 675–691.
- Archer, W. & Braun, D.R. (2013) Investigating the signature of aquatic resource use within Pleistocene hominin dietary adaptations. *PLoS One* **8**(8), e69899.
- Arriaza, M.C., Yravedra, J., Domínguez-Rodrigo, M. *et al.* (2017) On applications of micro-photogrammetry and geometric morphometrics to studies of tooth mark morphology: The modern Olduvai Carnivore Site (Tanzania). *Palaeogeography, Palaeoclimatology, Palaeoecology*. doi: 10.1016/j.palaeo.2017.01.036.
- Bartelink, E.J., Wiersema, J.M. & Demaree, R.S. (2001) Quantitative analysis of sharp-force trauma: an application of scanning electron microscopy in forensic anthropology. *J. Foren. Sci.* **46**, 1288–1293.
- Behrensmeyer, A.K., Gordon, K.D. & Yanagi, G.T. (1986) Trampling as a cause of bone surface damage and pseudo-cutmarks. *Nature* **319**, 768–771.
- Bello, S.M. (2011) New results from the examination of cut-marks using three-dimensional imaging. *The Ancient Human Occupation of Britain* (ed. by N. Ashton, S.G. Lewis & C. Stringer), pp. 249–262. Elsevier, Amsterdam, the Netherlands.
- Bello, S.M. & Soligo, C. (2008) A new method for the quantitative analysis of cutmark micromorphology. *J. Archaeol. Sci.* **35**, 1542–1552.
- Bello, S.M., Parfitt, S.A. & Stringer, C.B. (2009) Quantitative micromorphological analyses of cut marks produced by ancient and modern handaxes. *J. Archaeol. Sci.* **36**, 1869–1880.
- Bello, S.M., De Groote, I. & Delbarre, G. (2013) Application of 3-dimensional microscopy and micro-CT scanning to the analysis of Magdalenian portable art on bone and antler. *J. Archaeol. Sci.* **40**, 2464–2476.
- Bello, S.M., Saladié, P., Cáceres, I., Rodríguez-Hidalgo, A. & Parfitt, S.A. (2015) Upper Palaeolithic ritualistic cannibalism at Gough's Cave (Somerset, UK): the human remains from head to toe. *J. Human Evol.* **82**, 170–189.
- Bello, S.M., Wallduck, R., Dimitrijević, V., Živaljević, I. & Stringer, C.B. (2016) Cannibalism versus funerary defleshing and disarticulation after a period of decay: comparisons of bone modifications from four prehistoric sites. *Am. J. Phys. Anthropol.* **161**(4), 722–743.
- Binford, L.R. (1981) *Bones: Ancient Men, Modern Myths*. Academic Press, New York.
- Blasco, R., Rosell, J., Fernández Peris, J., Cáceres, I. & María Vergès, J. (2008) A new element of trampling: an experimental application on the level XII faunal record of Bolomor Cave (Valencia, Spain). *J. Archaeol. Sci.* **35**, 1605–1618.
- Blasco, R., Rosell, J., Smith, K.T., Maul, L.C., Sañudo, P., Barkai, R. & Gopher, A. (2016) Tortoises as a dietary supplement: a view from the Middle Pleistocene site of Qesem Cave, Israel. *Quarter. Sci. Rev.* **133**, 165–182.
- Blumenschine, R.J., Cavallo, J.A. & Capaldo, S.D. (1996) Meat eating, hominid sociality, and home bases revisited. *Curr. Anthropol.* **37**(2).
- Bonney, H. (2014) An Investigation of the use of discriminant analysis for the classification of blade edge type from cut marks made by metal and bamboo blades. *Am. J. Phys. Anthropol.* **154**, 575–584.
- Boschin, F. & Crezzini, J. (2012) Morphometrical analysis on cut marks using a 3D digital microscope. *Int. J. Osteoarchaeol.* **22**, 549–562.
- Bunn, H.T. (1981) Archaeological evidence for meat-eating by Plio-Pleistocene hominids from Koobi Fora, Kenya. *Nature* **291**, 574–577.
- Choi, K. & Driwantoro, D. (2007) Shell tool use by early members of *Homo erectus* in Sangiran, central Java, Indonesia: cut mark evidence. *J. Archaeol. Sci.* **34**, 48–58.
- Core-Team, R. (2015) *A language and Environment for Statistical Computing*. R Foundation for Statistical Computing, Vienna, Austria. URL <https://www.Rproject.org/>.
- Crezzini, J., Boschin, F., Boscato, P. & Wierer, U. (2014) Wild cats and cut marks: exploitation of *Felis silvestris* in the Mesolithic of Galgenbühel/Dos de la Forca (South Tyrol, Italy). *Quarter. Int.* **330**, 52–60.
- Cruz Uribe, K. & Klein, R.G. (1994) Chew marks and cut marks on animal bones from the Kastelberg B and Dune field Midden Later Stone Age sites, Western Cape Province, South Africa. *J. Archaeol. Sci.* **21**, 35–49.
- Dawkins, W. & Boyd, H. (1874) *Cave Hunting Research of the Evidence of Caves Respecting the Early Inhabitants of Europe Early Man in Britain*. Macmillan & Co., London.
- De Juana, S., Galán, A.B. & Domínguez-Rodrigo, M. (2010) Taphonomic identification of cut marks made with lithic handaxes: an experimental study. *J. Archaeol. Sci.* **37**, 1841–1850.
- Domínguez-Rodrigo, M. (1997a) Meat eating by early hominids at FLK Zinj 22 Site, Olduvay Gorge Tanzania: an experimental a roach using cut-mark data". *J. Human Evol.* **33**, 669–690.
- Domínguez-Rodrigo, M. (1997b) A Reassessment of the study of cut marks patterns to infer hominid manipulation of fleshed carcasses at the FLK Zinj 22 Site, Olduvay Gorge Tanzania. *Trabajos de Prehistoria* **54**(2), 29–42.
- Domínguez-Rodrigo, M. (1997c) Meat eating and carcass procurement by hominids at the FLK Zinj 22 site Olduvai Gorge Tanzania. A new experimental a roach to the old hunting-versus-scavenging debate. *Lifestyles and Survival Strategies in Pliocene and Pleistocene Hominids* (ed. by H. Ullrich), pp. 89–111. Edition Archaea, Schwelm Germany.
- Domínguez-Rodrigo, M., Barba, R. & Egeland, C.P. (2007) *Deconstructing Olduvai: A Taphonomic Study of the Bed I Sites*. Springer Books, the Netherlands.
- Domínguez-Rodrigo, M., de Juana, S., Galán, A.B. & Rodríguez, M. (2009) A new protocol to differentiate trampling marks from butchery cut marks. *J. Archaeol. Sci.* **36**, 2643–2654.
- Domínguez-Rodrigo, M., Bunn, H.T. & Pockering, T.R. (2010) Configurational approach to identifying the earliest hominin butchers. *Proc. Nat. Acad. Sci.* **107**(49), 20929–20934.
- Domínguez-Rodrigo, M. & Yravedra, J. (2009) Why are cut mark frequencies in archaeofaunal assemblages so variable? A multivariate analysis. *J. Archaeol. Sci.* **36**, 884–894.
- Dryden, I.L. & Mardia, K.V. (1998) *Statistical Shape Analysis*. Wiley, Chichester.

- During, E.M. & Nilsson, L. (1991) Mechanical surface analysis of bone: a case study of cut marks and enamel hypoplasia on a Neolithic cranium from Sweden. *Am. J. Phys. Anthropol.* **84**, 113–125.
- Efremov, L.A. (1940) Taphonomy a new branch of Paleontology Pan. *Am. Geol.* **74**(2), 81–93.
- Güth, A. (2012) Using 3D scanning in the investigation of Upper Palaeolithic engravings: results of a pilot study. *J. Archaeol. Sci.* **39**(10), 3105–3114.
- Fraser, C. (1980) Multiple focal setting self-calibration of close-range metric cameras. *Photogr. Eng. Remote Sens.* **46**, 1161–1171.
- Fiorillo, A.R. (1989) An experimental study of trampling: Implications for the fossil record. In *Bone Modification*, (eds. by R. Bonnichsen & M. Sorg), pp. 61–72. Center for the Study of the First Americans, Orono, ME.
- Fisher, D.C. (1995) Bone surface modifications in zooarchaeology. *J. Archaeol. Method Theor.* **2**, 7–68.
- Galán, A.B. & Domínguez-Rodrigo, M. (2013) An experimental study of the Anatomical distribution of cut marks created by filleting and disarticulation on the long bone ends. *Archeometry* **55**, 1132–1149.
- Gilbert, W.H. & Richards, G.D. (2000) Digital imaging of bone and tooth modification. *Anatom. Rec.* **261**, 237–246.
- Greenfield, H.J. (1999) The origins of metallurgy: distinguishing stone from metal cut-marks on bones from archaeological sites. *J. Archaeol. Sci.* **26**, 797–808.
- Greenfield, H.J. (2004) The butchered animal bone remains from Ashqelon, Afridar-Area G. *Antiqot* **45**, 243–261.
- Greenfield, H.J. (2006a) The butchered animal bones from Newe Yam, a submerged pottery Neolithic site off the Carmel Coast. *J. Israel Prehist. Soc.* **36**, 173–200.
- Greenfield, H.J. (2006b) Slicing cut marks on animal bones: diagnostics for identifying stone tool type and raw material. *J. Field Archaeol.* **31**, 147–163.
- González-Aguilera, D., López-Fernández, L., Rodríguez-González, P. et al. (2016a) Development of an all-purpose free photogrammetric tool. Congress: Development of an all-purpose free photogrammetric tool. Date: 12 to 19 of July of the year 2016, Prague, Czech Republic.
- González-Aguilera, D., López-Fernández, L., Rodríguez-González, P. et al. (2016b) InteGRATED PHOtogrammetric Suite, GRAPHOS. Congress: CATCON7-ISPRS. Date: 12 to 19 of July of the year 2016, Prague, Czech Republic.
- Harlé, E. (1892) Presentation del os provenant de rapas de Hyenes tachetees. *Bull. Soc. Hist. Nat. Toulouse. T. XXVI.* 22–25.
- Kaiser, T.M. & Katterwe, H. (2001) The application of 3D-Microprofilometry as a tool in the surface diagnosis of fossil and sub-fossil vertebrate hard tissue. An example from the Pliocene Upper Laetoli Beds, Tanzania. *Int. J. Osteoarchaeol.* **11**, 350–356.
- Klingenberg, H. (2011) MorphoJ: an integrated software package for geometric morphometrics. *Mol. Ecol. Resour.* **11**, 353–357.
- Knox, H. (1822) *Notice Relevant to the Habits of Hyaena in Southern Africa*, pp. 1–383. Transitions of the Wernerian Natural history Society, Edinburgh.
- Lartet, E. (1860) On the coexistence of man with certain extinct quadrupeds, proved by fossil bones from various Pleistocene deposits, bearing incisions made by sharp instruments. *Quart. J. Sociolog. Soc. Lond.* **16**, 471–479.
- Lartet, E. & Christy, H. (1875) *Reliquiae Aquitanicae Being Contributions to the Archaeology and Paleontology of Perigord and Adjoining Provinces of Southern France*. London Williams and Nagorte, London.
- Lewis, J.E. (2008) Identifying sword marks on bone: criteria for distinguishing between cut marks made by different classes of bladed weapons. *J. Archaeol. Sci.* **35**, 2001–2008.
- Lupo, K.D. & O'Connell, J.F. (2002) Cut and tooth mark distributions on large animal bones: ethnoarchaeological data from the Hadza and their implications for current ideas about early human carnivore. *J. Archaeol. Sci.* **29**, 85–109.
- Lyman, R.L. (1987) Archaeofaunas and butchery studies: a taphonomic perspective. *Advances in Archaeological Method and Theory* (ed. by M. Schiffer), vol. **10**, pp. 249–337. Springer, New York.
- Nilsen, P.J. (2001) An actualistic butchery study in South Africa and its implications for reconstructing hominid strategies of carcass acquisition and butchery in the Upper Pleistocene and Plio-pleistocene. PhD Dissertation, University of Cape Town.
- Marín-Monfort, M.D., Pesquero, M.D. & Fernández-Jalvo, Y. (2014) Compressive marks from gravel substrate on vertebrate remains: a preliminary experimental study. *Quarter. Int.* **330**, 118–125.
- Maté-González, M.A., Yravedra, J., González-Aguilera, D., Palomeque-González, J.F. & Domínguez-Rodrigo, M. (2015) Micro-photogrammetric characterization of cut marks on bones. *J. Archaeol. Sci.* **62**, 128–142.
- Maté-González, M.A., Palomeque-González, J.F., Yravedra, J., González-Aguilera, D. & Domínguez-Rodrigo, M. (2016) Micro-photogrammetric and morphometric differentiation of cut marks on bones using metal knives, quartzite and flint flakes. *Archaeol., Anthropol. Sci.* **0**, 1–12. DOI 10.1007/s12520-016-0401-5.
- Martin, H. (1906) Presentation d'ossement de rene pertante des lesions d'origine humaine et animale. *Bull. Soc. Préhist. Fran.* **3**, 385–397.
- Martin, H. (1907–10). *Recherches sur l'évolution du Musterien dans le gisement de la Quina (Charente)*. Vol. Industrie Osseuse. Paris Schleicher Freres.
- Martin, H. (1909) Desarticulation des quelques regions chez les ruminants et le cheval a l'époque moustérienne. *Bull. Soc. Préhist. Fran.* **7**, 303–310.
- Montani, L., Sapin, E., Sylvestre, R. & Marquis, R. (2012) Analysis of roman pottery graffiti by high resolution capture and 3D laser profilometry. *J. Archaeol. Sci.* **39**(11), 3349–3353.
- Olsen, S.L. (1988). *The Identification of Stone and Metal Tool Marks on Bone Artefacts BAR*, vol. 452, pp. 337–360. British Archaeological Reports, Oxford.
- Olsen, S.L. & Shipman, P. (1988) Surface modification on bone: trampling vs butchery. *J. Archaeol. Sci.* **15**, 535–553.
- Pante, M.C., Muttart, M.V., Keevil, T.L., Blumenschine, R.J., Njau, J.K. & Merritt, S.R. (2017) A new high-resolution 3-D quantitative method for identifying bone surface modifications with implications for the Early Stone Age archaeological record. *J. Human Evol.* **102**, 1–11.
- Rohlf, F.J. (1999) Shape statistics: procrustes superimpositions and tangent spaces. *J. Classific.* **16**, 197–223.
- Shipman, P. (1981) Life historia of a fossil. *An Introduction to Taphonomy and Paleoecology*. Harvard University Press.
- Shipman, P. (1988) Actualistic studies of animal and hominid activities. *The Identification of Stone and Metal Tool Marks on Bone Artifacts BAR* (ed. by S.L. Olsen), vol. 452, pp. 261–285, 337–360. British Archaeological Reports, Oxford.
- Shipman, P. & Rose, J. (1983) Early hominid hunting, butchering and carcass-processing behaviours: a roaches to the fossil record. *J. Anthropol. Archaeol.* **2**, 57–98.

- Slice, D.E. (2001) Landmark coordinates aligned by procrustes analysis do not lie in Kendall's shape space. *Syst. Biol.* **50**(1), 141–149.
- Smith, M.J. & Brickley, M.B. (2004) Animals and interpretation of flint toolmarks found on bones from West Tump Long Barrow, Gloucestershire. *Int. J. Osteoarchaeol.* **14**, 18–33.
- Spennerman, D.H.R. (1990) Don't forget the bamboo on recognising and interpreting butchery marks in tropical faunal assemblages some comments asking for caution. *Problems Solving Taphonomy Tempus* (ed. by S. Solomon, I. Davidson & D. Watson), vol. 2, pp. 80–101. Tempus.
- Thirria, E. (1833) Statique minéralogique et géologie du département de la Haute-Loire Besançon Outhenin Chalande.
- Tournal, M. (1833) General considerations on the phenomenon of bone awrens. *Ann. Chimie Phys.* **25**, 161–171
- Walker, P.L. (1978) Butchering and stone tool function. *Am. Antiq.* **43**(4), 710–715.
- Walker, P.L. & Long, L.C. (1977) An experimental study of the morphological characteristics of tool marks. *Am. Antiq.* **42**, 605–616.
- West, J. & Louys, J. (2007) Differentiating bamboo from stone tool cut marks in the zooarchaeological record, with a discussion on the use of bamboo knives. *J. Archaeol. Sci.* **34**, 512–518.
- White, T.E. (1952) Observations on the butchering technique of some aboriginal peoples. 1. *Am. Antiq.* **17**, 337–338.
- White, T.E. (1953) Observations on the butchering technique of some aboriginal peoples. 2. *Am. Antiq.* **19**, 160–164.
- White, T.E. (1954) Observations on the butchering technique of some aboriginal peoples. 3, 4, 5, 6. *Am. Antiq.* **19**, 254–264.
- White, T.E. (1955) Observations on the butchering technique of some aboriginal peoples. 7, 8, 9. *Am. Antiq.* **21**, 170–178.
- Yravedra, J., Morín, J., Agustí, E. *et al.* (2009) Implicaciones Metalúrgicas de las marcas de corte en la transición Bronce Final-Hierro en el interior de la Península Ibérica. *Gallaecia* **28**, 77–92.
- Yravedra, J., Maté-González, M.Á., Palomeque-González, J.F. *et al.* (2017) A new approach to raw material use in the exploitation of animal carcasses at BK (Upper Bed II, Olduvai Gorge, Tanzania): a micro-photogrammetric and geometric morphometric analysis of fossil cut marks. *Boreas* DOI 10.1111/bor.12224.

### Supporting Information

Additional Supporting information may be found in the online version of this article at the publisher's website:

**Fig. S1.** Inventory with photographs and sections of cut marks.